Catalytic Upgrading of Rice Straw Bio-Oil via Esterification in Supercritical Ethanol Over Bimetallic Catalyst Supported on Rice Straw Biochar

Alhassan Ibrahim , Islam Elsayed , El Barbary Hassan *

Posted Date: 14 December 2023

doi: 10.20944/preprints202312.1065.v1

Keywords: Rice straw; Fast pyrolysis; Biochar; Bio-oil upgrading; Bimetallic oxide catalysts

Article

Catalytic Upgrading of Rice Straw Bio-Oil via Esterification in Supercritical Ethanol over Bimetallic Catalyst Supported on Rice Straw Biochar

Alhassan Ibrahim [1], Islam Elsayed [1,2] and El Barbary Hassan [1,*]

[1] Department of Sustainable Bioproducts, Mississippi State University, Mississippi State, MS 39762, USA
[2] Department of Chemistry, Faculty of Science, Damietta University, New Damietta, Egypt
* Correspondence: e.hassan@msstate.edu

Abstract: This research explores the enhancement of bio-oil quality through upgrading with the magnetic bimetallic oxide (CuO-Fe_3O_4) catalysts supported on activated rice straw biochar (AcB). These catalysts were employed in a supercritical ethanol-based upgrading process. Various characterization techniques, including elemental analysis, XRD, BET, TGA, and SEM, were utilized to characterize the prepared catalyst. The study revealed significant improvements in the physical characteristics and chemical composition of the bio-oil, with higher heating value (HHV) increasing from 21.3 to 32.1 MJ/kg. Esterification and transesterification were identified as key reactions contributing to this improvement. Notably, the pH of bio-oil increased from 4.3 (raw bio-oil) to 5.63 (after upgrading), signifying reduced acidity. The analysis of the bio-oil's chemical composition highlighted a decrease in oxygen content and an increase in carbon and hydrogen content. At the optimum conditions, the application of supercritical ethanol proved to be an efficient method for enhancing the bio-oil's properties. A crucial transformation occurred during the upgrading process and more than 90% of carboxylic acids were converted into esters, primarily ethyl acetate at the optimal conditions. This study has demonstrated the effective enhancement of raw bio-oil from rice straw through the utilization of carbon-based bimetallic oxide catalysts in a supercritical upgrading procedure.

Keywords: rice straw; fast pyrolysis; biochar; bio-oil upgrading; bimetallic oxide catalysts

1. Introduction

The rapid depletion of fossil fuels, coupled with the environmental threat it poses as a result of greenhouse gases emissions, has triggered the search for an alternate and sustainable source of fuels from lignocellulosic biomass [1]. Lignocellulosic biomass fuel has enormous advantages over the current fossil fuel due to its negligible sulfur content, renewability, and lower greenhouse gas emission of 80-90% [2]. By 2022, the United States estimated 360 billion gallons of the world's total fuel consumption would be made up of renewable resources. Wood and agricultural residues are the most common sources of renewable resources [3]. Agricultural residues, including rice straw, are some of the most abundant and least costly lignocellulosic biomasses, accounting for about 283 million tons annually worldwide [4]. Consequently, their effective utilization can significantly lead to a major reduction of gas emissions. At the same time, their utilization will represent an additional source of renewable biofuels [5]. Rice straw biomass from one of the world's most consumed foods is gaining more attention for bio-oil production through fast pyrolysis technique under both catalytic and non-catalytic conditions [6].

Fast pyrolysis is a thermochemical process which can produce a liquid fuel that may be used to replace fossil fuels in any static heating or electrical generation applications [7]. The fast pyrolysis process thermally degrades the biomass into liquid bio-oil, mixture of gases, and solid biochar in the absence of air at a temperature of (400-450°C) and pressure of (0.1-0.5 MPa). Over the years, a great deal of work has gone into developing pyrolysis processes for creating high bio-oil yield from

lignocellulosic biomass [8]. The major challenges with fast pyrolysis bio-oil, irrespective of the biomass source, are the bio-oil chemical composition. Bio-oil typically consist of a complex mixture of organic compounds such as acids, alcohols, aldehydes, esters, ketones, sugars, guaiacols, syringols, furans, lignin derived phenols, levoglucosans and other compounds [9]. The presence of a high-water content and the high percentage of oxygenated compounds (35-40 wt.%) are the main reasons for bio-oil negative properties such as low heating value ranging (13-20 MJ/kg) and immiscibility with fossil fuels [10]. Additionally, bio-oil has a strong tendency to polymerize during storage and transit and contains substantial quantities of carboxylic acids, such as formic, propanoic, and acetic acids, which results in low pH values (2-3) and makes bio-oil more corrosive [11]. Therefore, the development of suitable upgrading techniques for decreasing the acid value, oxygen-containing species, increasing the calorific value, and stabilizing bio-oil is highly required for the ultimate utilization of fast pyrolysis bio-oil [12].

Several upgrading techniques, such as hydrogenation, hydrodeoxygenation (HDO), catalytic cracking, emulsification, and esterification in supercritical fluids have been developed to improve the physicochemical properties of fast pyrolysis bio-oil [13]. The esterification process to transform the enormous quantities of carboxylic acids that exist in the bio-oil, such as formic acid, acetic acid, and propionic acid can be achieved by using alcohols which led to reduction in the acidic value and thus addressing the corrosive nature of the bio-oil [14]. The esterified bio-oil represents a greener approach to ester production which can be essentially used as biodiesel [15]. The esterification process can be performed in the presence of a liquid homogeneous acid catalyst or a solid acid catalyst. The esterification process with a heterogenous solid catalyst alongside the HDO is seen as the best approach for bio-oil upgrading [14]. It is also important to note that esterification carried in the presence of a solid heterogenous catalyst does not only catalyze the esterification reaction but also aid the deoxygenation of the esterified bio-oil, thereby further enhancing the calorific value upgraded fuel [16]. It is therefore not surprising that, lately, there has been a development in the enhancement of fast pyrolysis bio-oils through supercritical alcohol treatment, presenting an alternative to traditional techniques like HDO and catalytic cracking [17,18].

This novel approach of utilizing supercritical alcohol for upgrading via esterification using a heterogenous catalyst offers a promising solution to tackle the common issues of hydrogen availability and coke formation encountered in conventional bio-oil upgrading methods [19,20]. The demand for hydrogen in the other upgrading technique, such as the HDO process, can be fulfilled by a hydrogen transfer from the supercritical alcohol with the help of the catalyst [19,21]. The distinctive characteristics of supercritical alcohols as solvents creates a unified reaction environment by dissolving gases, such as hydrogen, after dissociation [18]. This setup facilitates the HDO reaction by eliminating mass transfer barriers and curbs the formation of coke by stabilizing the precursors that lead to coking [22]. Ethanol, among various alcohols, has gained significant attention as an optimal solvent for supercritical upgrading because alcohols are cheaper, safer, and more appropriate to use as a hydrogen donor than molecular H_2 [22,23]. This preference is attributed to its exceptional capability to dissolve organic compounds within the bio-oil, along with its origin from biomass. Furthermore, the application of supercritical ethanol aids in minimizing waste production during the upgrading procedure [24]. Moreover, the alcohols employed in this process exhibit heightened efficiency in esterification reactions, effectively stabilizing the acidic components present in the bio-oil [25,26].

HDO of bio-oils has extensively been studied using the conventional petroleum hydrotreating catalysts, such as noble metals Rh, Pd, and Pt were used [27]. Though noble metals have demonstrated notable catalytic efficacy in HDO, yet their substantial production expenses impose restrictions on their practical application [28]. In contrast, transition metals like Ni, Cu, Fe, Co, and Mo, while more cost-effective, tend to exhibit comparatively reduced catalytic activity in HDO [29,30]. Other combinations of bimetallic CoMo, NiMo supported on alumina were also studied [31,32]. The bimetallic NiCo catalysts were also used in the deoxygenation of palm oil to methyl ester [33]. Of all the above discussed transition metals, Cu and Fe are not only cheaper and abundantly available but also comparably the least studied.

 doi:10.20944/preprints202312.1065.v1

Besides the activities of metal loading in catalysts, the type of support also plays critical role in bio-oil upgrading. Several supports, including biochar, metal oxides, and zeolites, had reportedly been used as catalyst supports for chemical biomass conversion to bio-oil [34–36]. Additionally, it was found that acidic catalysts like zeolites and silica-alumina work effectively in upgrading bio-oil even under atmospheric pressure without needing hydrogen [42]. Though all these catalyst supports have been proven to be effective in bio-oil upgrading, biochar-based support catalysts is more cost-effective, readily available, and environmentally benign [37]. The homologous biochar-supported inlaid Cu–Ni catalysts were used for lignin depolymerization to monophenols and bio-oil without the use external hydrogen [38]. In a few instances, trimetallic catalysts, such as MgNiMo supported on activated charcoal, were used successfully for bio-oil esterification under supercritical ethanol conditions [14]. It is worth noting that most of these biochar-based catalysts were prepared using commercially purchased activated carbon, some of which had been utilized for the purpose of upgrading bio-oil derived from fast pyrolysis in supercritical ethanol [14,39]. It is therefore not surprising that recently biochar has become more popular catalyst support like zeolite, alumina, oxides etc. On the other hand, activated biochar is a reliable resource for organic carbon-based supports which makes a not only sustainable and environmentally friendly, but also a cheaper alternative to zeolite, alumina, and other commercial options etc. [40,41].

Rice straw biochar in the form of activated biochar was used as a support due to its unique chemical composition, such as higher silica content and morphological characteristics, allowing for successful loading of metal oxides such as Fe_3O_4 and CuO on its acid sites compared to biochar form other biomass sources [42,43]. Therefore, this study will focus primarily on the synthesis and characterization of the magnetic bimetallic oxide catalysts supported on the activated rice straw biochar (CuO-Fe_3O_4/AcB) and using it for the catalytic upgrading of rice straw bio-oil under supercritical ethanol conditions. The prepared catalyst will be characterized with X-ray diffraction (XRD), BET Surface area, and pore size distribution by BJH, elemental analyzer, thermogravimetric analysis (TGA), and scanning electron microscope (SEM). The esterified upgraded bio-oil will be characterized by the commonly physical and chemical characterization methods.

2. Materials and Methods

2.1. Materials

Rice Straw feedstock was collected from Delta Research and Extension Center (DREC) at Stoneville, MS. The metal precursors, such as Copper (II) nitrate trihydrate Cu $(NO_3)_2.3H_2O$ and iron (III) nitrate nonahydrate $Fe_2(NO_3)_3.9H_2O$, were purchased from Fisher Scientific with a percent purity of ≥ 99%. Sodium hydroxide (NaOH) and potassium bicarbonate (K_2CO_3) were obtained from Millipore-Sigma. Methanol, ethanol, and acetone with a percent purity ≥99% were purchased from Fisher Scientific and used without further purification.

2.2. Pyrolysis of Rice Straw

Schematic diagram of the overall pyrolysis and upgradation processes are presented in Figure 1. The pyrolysis of rice straw was conducted at a feed rate of approximately 7 kg/h within a stainless-steel auger reactor, as described in our previous publication [44]. The operation of the auger reactor excluded the use of a carrier gas or additional heat carrier, relying instead on nitrogen to eliminate oxygen from the system. Pyrolysis was achieved by maintaining a pyrolysis temperature of 425 °C, with a calculated gas residence time falling within the range of 1-2 seconds. Multiple heaters, situated along the reactor pipe, were responsible for supplying the requisite heat for the pyrolysis reactions. During the experimental process, the solid feed material took approximately 30 seconds to traverse the 450 °C pyrolysis zone, with a total transit time of approximately 50 seconds to reach the char exit point. The resulting pyrolysis vapors were subsequently conveyed through the pipe into a condenser train, where they underwent condensation to yield liquid bio-oil. The condenser system was designed to recover multiple liquid fractions from the pyrolysis vapors. The non-condensable gases generated within this process were collected at the end of the condenser train using a gas sampling

Preprints (www.preprints.org) | NOT PEER-REVIEWED | Posted: 14 December 2023 doi:10.20944/preprints202312.1065.v1

bag and a gas sampler kit (GAV-200 MK 2, SGE Inc., Austin, TX). Liquid condensate resulting from the condensation process was collected from the exits of four condensers and subsequently assembled to form a composite bio-oil sample. The biochar, a solid byproduct of pyrolysis, was collected within a sealed vessel positioned at the end of the reactor tube, with the weights of the biochar samples being diligently recorded.

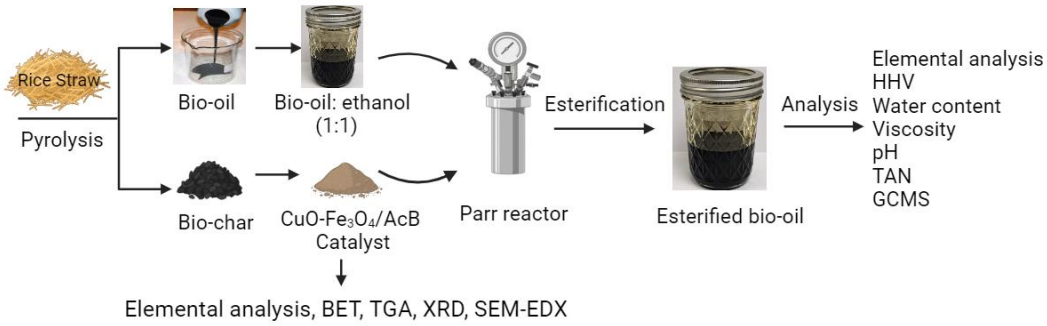

Figure 1. Schematic diagram of the experimental set up for pyrolysis and upgrading processes.

2.3. Preparation of biochar-based catalysts

The activated rice straw biochar (AcB) was prepared according to following procedure [45]. 100 g biochar was impregnated in 300 mL of 0.6 M K_2CO_3 solution for 24 h. The mixture was stirred for 48 hrs. using a magnetic stirrer. The impregnated biochar was separated by centrifuge and dried at 80 °C in the oven, then pyrolyzed using in a furnace tube (OTF-1200X) with a heating rate of 10 °C/min under inert condition using nitrogen gas. The heating temperatures was set to 600 °C for 2 h. The obtained activated biochar was grinded to pass a 0.15 mm sieve, then treated with 1 M HCl to remove ash and washed with deionized water until the conductivity of the washed filtrate became less than 10 µS/cm. At the end, the activated biochar was vacuum dried at 80 °C and kept covered.

2.4. Preparation of CuO-Fe_3O_4/AcB

Five different combinations of the (CuO-Fe_3O_4/AcB) biochar-based catalysts (1, 2, 3, 4, and 5) were prepared using the precipitation-deposition method with slight modifications [46]. The weight of activated biochar was added to 250 mL of deionized water then sonicated for 30 min at room temperature to obtain a good dispersion. The required weight of (Cu) in the form of Cu $(NO_3)_2.3H_2O$ and (Fe) in the form of $Fe_2(NO_3)_3.9H_2O$ were weighed and dispersed in 250 mL water and sonicated for 10 min for complete dissolution. Then the metal-nitrate mixtures were added into the activated biochar dispersion drop-wise with constant stirring using a mechanical stirrer. Following this, both metals were precipitated by using 1.0 M NaOH at 0 °C using ice with keeping the suspension pH fixed at 9.5 by monitoring with a pH meter. The suspension was then stirred at room temperature for 1 h and filtered using a centrifuge, then washed with deionized water continuously until the detection of a neutral pH of the filtrate. Afterwards, the residue was put into vacuum oven and allowed to dry overnight at 80°C. The precipitate was then calcined in a furnace tube (OTF-1200X) at 550 °C for 5 hrs. in air. Finally, the obtained catalyst was reduced at 400 °C under 5% H_2 in N_2 flow (1 L/min) atmosphere for 5 h with a heating rate of 10 °C/min in a continuous flow in a furnace tube (OTF-1200X). Table 1 summarizes the different catalyst preparation conditions:

 doi:10.20944/preprints202312.1065.v1

Table 1. Conditions of the different prepared catalysts.

EXP.	Catalyst	AcB (wt%)	Cu and Fe (wt%)	Cu (wt%)	Fe (wt%)	Cu: Fe ratio
1	AcB	100	0	0	0	-
2	1	80	20	10	10	1:1
3	2	80	20	13.33	6.66	2:1
4	3	80	20	15	5	3:1
5	4	90	10	7.5	2.5	3:1
6	5	70	30	22.5	7.5	3:1

2.5. Catalyst Characterization

Characterization of the catalyst was performed by using different analytical techniques, such as TGA, XRD, SEM-EDX and Brunauer-Emmet-Teller (BET) analysis. The TGA (thermogravimetric analysis) of the AcB and CuO-Fe_3O_4/AcB catalyst was performed using the SDT Q600 TA instrument (USA). All measurements were made between 20 and 800 °C at a heating rate of 10 °C/min under N_2 atmosphere. X-Ray Diffraction (XRD) patterns for the prepared catalysts was determined with RINT Ultima III XRD (Rigaku Corp., Japan) operating with CuKα1 radiation (λ= 1.54 Å) at 40KV 44mA at the range of 3–90 (2θ) at 40 kV voltage and peak intensities were recorded every 0.03° at sweep rate of 1.0° (2θ/min). Scanning Electron Microscope (SEM) equipped with an Energy Dispersive X-Ray spectroscopy (SEM-EDX) was used to obtain the image of the morphology as well as the elemental composition (Cu, Fe, Si, O, and C) of the catalyst, and the two samples were sputter-coated with 15 nm platinum and imaged at a 5 keV accelerating voltage. The surface area (BET) and pore volume and size distribution (BJH) of the AcB and CuO-Fe_3O_4/AcB were determined by adsorption-desorption isotherms of nitrogen at −196 °C by using Quantachrome Autosorb iQ gas sorption analyzer (Quantachrome, USA).

2.6. Bio-oil esterification process

The bio-oil esterification process was carried out under a supercritical ethanol condition by first mixing bio-oil with ethanol in a ratio (1:1 w/w), and the bio-oil ethanol mixture was then used for the upgrading process. 100g of the bio-oil/ethanol mixture was taken for the catalytic upgrading process in a 350 mL Parr reactor equipped with a glass temperature controller, stirrer, and heating mantle. 5g weight of the catalyst was loaded in the reactor with the ethanol/bio-oil mixture. Then, the reactor was purged with N_2 for 5 times to remove the inside air. Subsequently, the reactor was heated to 300 °C at a heating rate of 5.0 °C/min. After 3 h, the heater was turned off and the reactor was cooled to the room temperature using an ice-water bath. The catalyst particles were separated from the liquid products in centrifuge vials by centrifugation at 4000 rpm for 30 min. The coke products along with the used catalysts were then recovered using vacuum filtration. The recovered solids were rinsed several times with acetone and dried at 105 °C for 12 h and weighed. The amount of coke formed during HDO process was calculated by subtracting the initial weight of catalyst from the total solids weight, assuming no catalyst loss. The aqueous fraction (AF) and oil fraction (OF) were unable to be separated since they were soluble in ethanol solvent. Thus, the OF was separated using a rotary evaporator to evaporate all the solvent and water at 65 °C under reduced pressure.

2.7. Physical and chemical characterization of raw and esterified bio-oil

The physical and chemical properties of rice straw bio-oil, such as pH, water content, viscosity, acid value, and heating value, were determined according to the appropriate standard methods. Water content was determined by the Karl Fisher titration method using a Cole-Parmer Model C-25800-10 titration apparatus (Thermo Fisher Scientific Inc., Waltham, MA) by ASTM D5291 method. Viscosities were determined by the Stabinger Viscometer TM SVM 3000 (Anton Parr, Austria) at 40 °C according to ASTM D7042 method. Total acid number (TAN) was obtained by dissolving a 1 g sample in 50 mL of 35:65 volume ratios of isopropanol to distilled water mixture and titrating to a

Preprints (www.preprints.org) | NOT PEER-REVIEWED | Posted: 14 December 2023 doi:10.20944/preprints202312.1065.v1

final pH of 8.5 with 0.1 N KOH solution by ASTM D664. Fourier transform infrared spectroscopy analysis was performed with a Perkin Elmer FTIR spectrometer. FTIR spectra was recorded in transmittance mode in the range of 4000-500 cm^{-1} with standard potassium bromide disk technique. Carbon, hydrogen, nitrogen, and oxygen (by difference) content were measured with a CE-440 Elemental Analyzer (Exeter Analytical, MA, USA) according to ASTM D3291 method with a standard of acetanilide (C=71.09 wt.%, H=6.71 wt.%, N=10.36 wt.% and O=11.84 wt.%). The higher heating value (HHV) was calculated in accordance with the DIN 51900 standard using Eq. (4). The volatile and semi-volatile components of each specimen were analyzed by a Perkin Elmer Clarus 500 Gas Chromatograph /Mass Spectrometer (GC/MS) system. The gas chromatograph was equipped with a DB-5MS capillary column of 30m x 0.32mm ID x 1 μm film thickness. Samples were injected in the split less mode and the injector temperature was 270 °C. The initial oven temperature of the GC was 40 °C for 4 min and then programmed at a rate of 5 °C/min to 280 °C, with a total run time of 60 min. The mass spectrometer detector was an electron impact ionization device operating at 70 eV with a source temperature of 210 °C and interface temperature of 225 °C. The chemical component data obtained from GC/MS was analyzed using a chemical integration program together with NIST mass spectral search library. The peak area percentage was calculated for each identified compound. However, compounds that were associated with some peaks were not identified.

$$HHV\ (MJ/kg) = \frac{(34 \times C + 124.3 \times H + 6.3 \times N + 19.3 \times S - 9.8 \times O)}{100} \quad (4)$$

(C, H, N, S, O was the elemental composition of the respective element)

3. Results

3.1. Catalyst Characterization

The textual properties of the synthesized (CuO-Fe_3O_4/AcB) bimetallic oxide catalyst and AcB support used in this study were determined by N_2 physisorption (BET and BJH methods) and summarized in Table 2. It is obvious that the metal loadings on the AcB support decreases the surface area and pore volume. However, the average pore diameter were inversely proportional to BET surface area, most likely due to the AcB pore being filled and blocked during the loading of metals oxide. The N_2 adsorption/desorption study of the bimetalic oxide catalyst (CuO-Fe_3O_4/AcB) in Figure 2 reveals a type IV N_2 adsorption/desorption isotherm with H3 hysteresis loop confirming the presence of meso and macro-porous material with plate-like layered structure. The catalyst shows a drop of BET surface area compared to the surface area of AcB support which could be due to the bimetallic oxide deposition on the surface of AcB.

Table 2. Textural properties of the prepared catalysts.

EXP. No.	Catalyst	BET Surface area (m^2/g)	Pore Volume (cc/g)	Average pore diameter (nm)
1	AcB	203.75	0.389	3.71
2	1	58.32	0.253	14.75
3	2	56.41	0.234	15.39
4	3	53.19	0.213	16.03
5	4	74.81	0.299	10.64
6	5	23.89	0.176	36.78

Preprints (www.preprints.org) | NOT PEER-REVIEWED | Posted: 14 December 2023 doi:10.20944/preprints202312.1065.v1

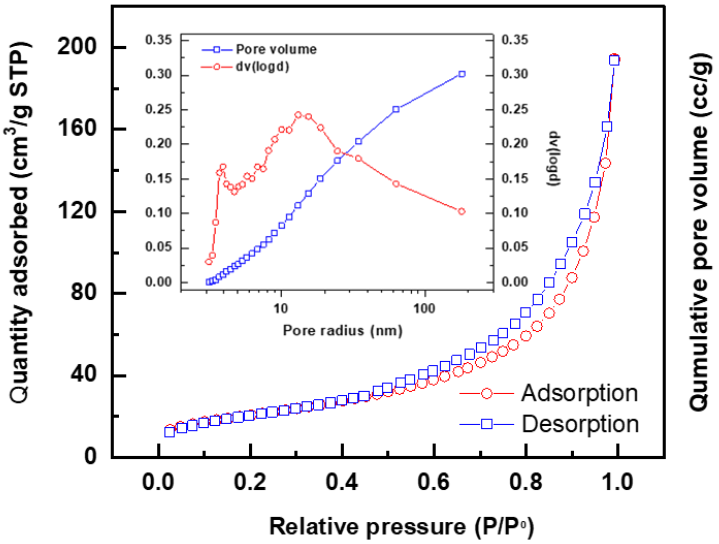

Figure 2. a. N_2 adsorption/desorption isotherms of CuO-Fe_3O_4/AcB catalyst (No. 4), and b. the pore size distribution.

The phase and the crystallinity of the prepared AcB support and CuO-Fe_3O_4/AcB catalyst were determined using XRD as well the average crystal size. As shown in Figure 3, the characterization spectrum of the AcB support was wide with a broad peak with no crystallinity, hence amorphous as expected. The XRD spectrum of the CuO-Fe_3O_4/AcB catalyst, on the other hand, shows crystallinity with a group of diffraction peaks at 2θ of 43.52°, 57.4° and 74.04° consistent with Fe_3O_4 were assigned to the cubic spinel unit cell that matches the standard magnetite structural data(JCPDS file no. 19-0629) [47]. These diffraction peaks of Fe_3O_4 400, 511, and 522 lattice planes confirm the existence of Fe_3O_4 . Also, A single cubic phase of Cu_2O, consistent with a standard cuprite structure with the diffraction peaks 111, 200, and 311 lattice planes, were found at 2θ of 38.5°, 42.4°, and 50.2° (JCPDS file no. 05-0667) [48]. Furthermore, diffraction peaks at 2θ of 38.5°, and 47.5°,and 52.3 consistent with CuO phase crystalline with monoclinic (tenorite) structure [48,49]. Hence the XRD has confirmed the presence of both metal oxides of CuO and Fe_3O_4 crystalline phases present in the synthesized CuO-Fe_3O_4/AcB catalyst.

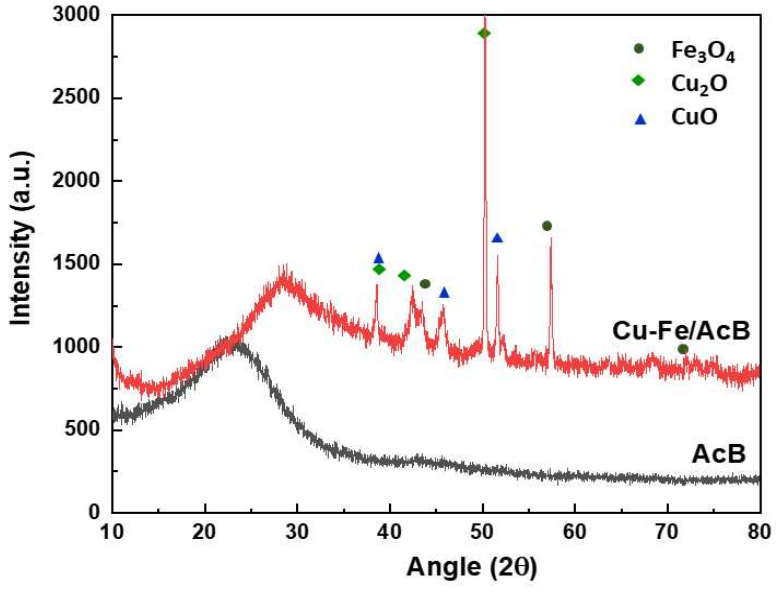

Figure 3. X-ray diffraction patterns of AcB and CuO-Fe_3O_4/AcB catalyst (No. 4).

Preprints (www.preprints.org) | NOT PEER-REVIEWED | Posted: 14 December 2023 doi:10.20944/preprints202312.1065.v1

Thermogravimetric analysis (TGA) was conducted on catalyst 4 under the presence of N_2 gas. This analysis aimed to determine the thermal stability and degradation within the catalysts. The outcomes of this analysis are presented in Figure 4. They experienced weight losses of (2.4%) from ambient temperature to 250 °C, which is mainly attributed to the removal of water. The catalyst exhibited higher thermal stability and less degradation tendency in the teperature range between 250- 600 °C. Hence, the catalyst most likely will remain stable throughout the reaction without degradation since our bio-oil upgrading process will mainly occure at temperature of 300 °C. The catalyst showed a slight weight loss of about (2.5%) beyound the activation temperature (600 °C) which is probably due to the degradtion of AcB compounds.

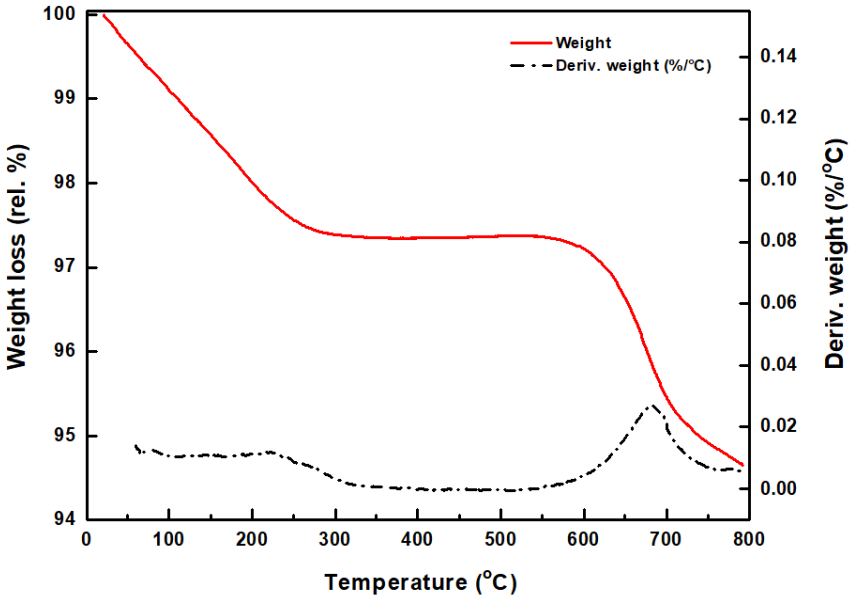

Figure 4. TGA of CuO-Fe_3O_4/AcB catalyst (No. 4).

SEM equipped with an EDX was used to to study the morphology as well as the elemental composition (Cu, Fe, Si, O, and C) of the catalyst as shown in Figure 5. The SEM images of the AcB support (a) appears as a sponge-like micropores structure while the image of the CuO-Fe_3O_4/AcB catalyst (b) shows the deposition of the metallic oxide crystal shape on the surface. The SEM-EDX elemental composition (c) spectra confirms the presence of bimetallic oxide loading of CuO-Fe_3O_4 and also worth noting is the peak of Si and O confirming the abundance of silica (Si-O-Si) in rice straw biochar [40] and the mapping d-h demonstrate that all metals oxide on the AcB support in the synthesized CuO-Fe_3O_4/AcB catalyst were well dispersed.

Preprints (www.preprints.org) | NOT PEER-REVIEWED | Posted: 14 December 2023 doi:10.20944/preprints202312.1065.v1

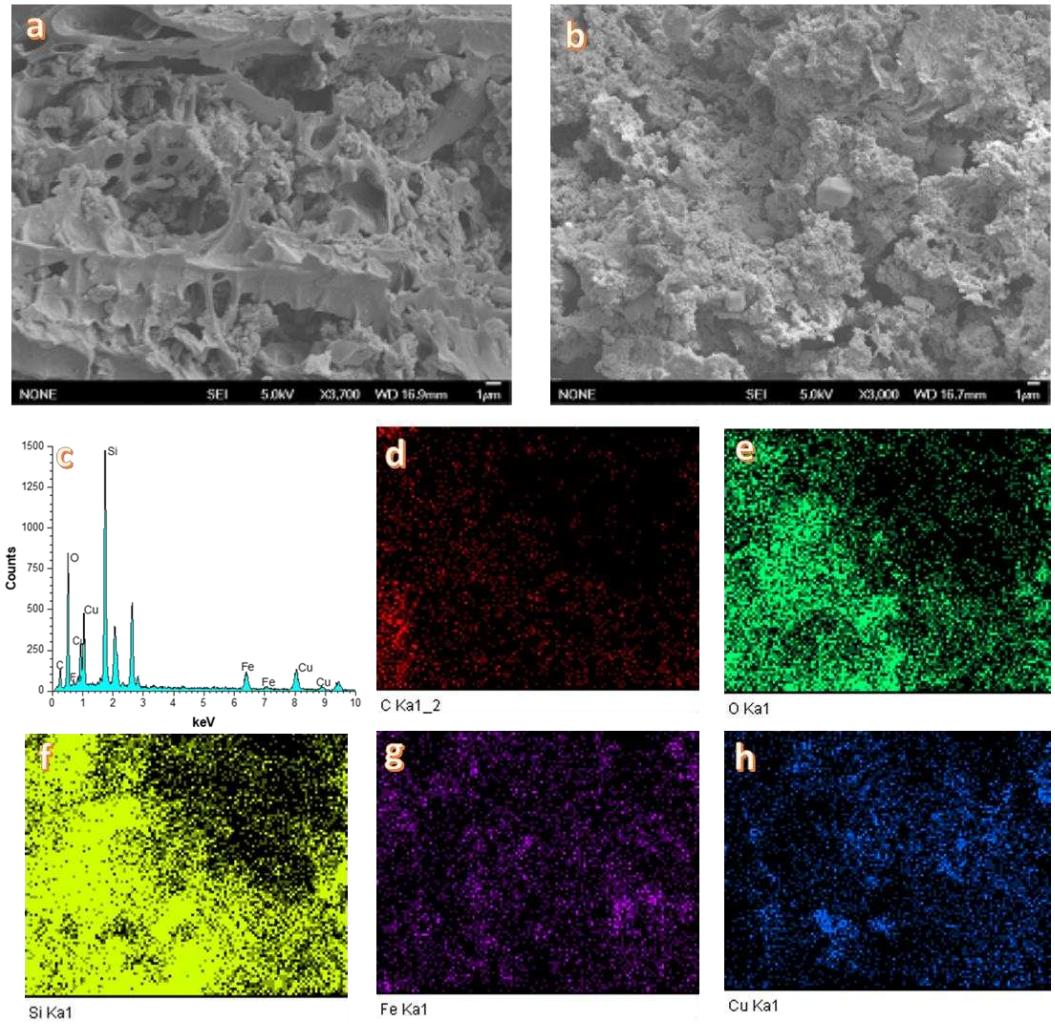

Figure 5. SEM-EDX of AcB and CuO-Fe_3O_4/AcB catalyst (No. 4).

3.2. Product yields, elemental analysis and HHV

The yields (Y) of the upgraded products (liquids, solids, and gas) were determined according to equations 1, 2, and 3 and presented in Table 2.

$$Y\ liquid\ = \frac{Mass\ (liquid)}{Mass\ (bio-oil+ethanol)} \times 100\ \%\ (1)$$

$$Y\ solid\ = \frac{Mass\ (solid)}{Mass\ (bio-oil+ethanol)} \times 100\ \%\ (2)$$

$$Y\ gas\ = 1 - \text{Yield (Liquid + Solid)} \times 100\ \%\ (3)$$

In the absence of a catalyst (Exp. 1), the yield of liquid products (56.3%) was relatively higher than the yields of liquid products (36.0-38.4%) in experiments performed in the presence of the catalyst (Exps. 2-6). Also, the yield of solids (4.3%) was relatively lower than that in the presence of a catalyst (17.3- 19.6%). The above results clearly indicate that the presence of a catalyst had a great influence on the product yields of liquid, solid, and accordingly, gas. The elemental composition of raw and esterified bio-oils with different catalysts was investigated as well in Table 3. As per the upgrading procedure, there has been an increase in the carbon (C) content and a decrease in the oxygen (O) content. Due to the increased (C) content and decreased (O) concentration, the esterified bio-oils exhibited Higher Heating Values (HHVs) than raw bio-oil. In Exp. 1, when the bio-oil was upgraded even with the absence of the bimetallic oxide catalyst, the HHV was increased to 24.3 (MJ/kg) compared to raw bio-oil 21.3 (MJ/kg) indicating the ability of the silica-rich biochar (AcB) alone to act as catalyst due to the presence of silica [41]. Replacing 20% AcB with metals (Exp. 2, and

Preprints (www.preprints.org) | NOT PEER-REVIEWED | Posted: 14 December 2023 doi:10.20944/preprints202312.1065.v1

3) lead to a pronounce increase in both carbon content (62.3 and 62.9%) and heating value (27.8, and 28.9 MJ/kg). The increase in the HHV was more obvious in Exp. 3 when the ratio of Cu:Fe loading was 2:1. Increasing the ratio of Cu:Fe to (3:1) in the catalyst (Exps. 4,5,6) leads to more improvement in both carbon content and HHV. The maximum HHV of 32.1 MJ/kg which represented about 49.8% increase in the HHV of raw bio-oil was achieved in Exp. 5.

Table 3. Product yield and elemental analysis results for raw and upgraded bio-oil.

EXP. No.	Y (liquid)	Y (solid)	Y (gas)	Elemental Analysis (wt.%)				HHV (MJ/kg)
				C	H	N	O	
Raw bio-oil	-	-	-	54.2	7.7	1.8	36.3	21.3
1	56.3	4.3	39.4	60.7	7.2	2.1	28.0	24.3
2	37.4	17.6	45.0	62.3	7.6	2.2	27.9	27.8
3	38.4	17.3	44.3	62.9	6.6	3.1	27.4	28.9
4	36.0	19.1	44.9	65.4	9.1	2.8	22.7	30.9
5	37.4	19.3	43.3	66.9	9.1	2.2	21.8	32.1
6	36.9	19.6	43.5	67.0	8.8	3.3	20.9	31.9

(Upgrading Temp. = 300 °C, time = 3h, bio-oil/ethanol mixture = (1: 1 w/w)).

3.3. Physical chractarization of raw and esterified upgraded bio-oils

Rice straw bio-oil, like other bio-oils, is composed of a complex mixture of oxygenated compounds, with the majority being carboxylic acids. The other oxygenated compounds primarily consist of alcohols, aldehydes, phenols, and ketones, among others [50]. The upgrading of rice straw bio-oil in supercritical ethanol primarily leads to the formation of esters through esterification reactions between ethanol and carboxylic acids. Table 4. represents physical properties of both raw and upgraded bio-oil. It is not so surprising that desirable biofuel properties, such as the lowest water content, least viscosity, and density, are associated with Exp. 5. Notably, Exp. 5 boasts the highest pH value of 5.6, rendering it the least acidic in comparison to raw bio-oil, Exp. 4 and Exp. 6, which feature pH values of 4.3, 4.9, and 4.7, respectively. This result has a strong correlation with the total acid number (TAN) values. The TAN value of Exp.5 was significantly decreased by 28.1% in comparison to raw bio-oil. This decrease in acid number is mainly related to the esterification of the carboxylic acid compounds in the raw bio-oil. In general, all upgraded bio-oils experiments showed lower TAN values, viscosity, water content, and density compared to raw bio-oil confirming the significant improvement in the physical properties of the esterified bio-oil.

Table 4. Physical properties for raw and upgraded bio-oil.

EXP. No.	Water content	Viscosity at 40 °C Cst	Density at 40 °C (g/cm³)	pH	TAN (mg KOH/g)
Raw bio-oil	38.5	1.88	0.92	4.3	83.9
1	35.2	1.78	0.87	4.6	75.7
2	34.4	1.68	0.84	4.8	74.5
3	34.0	1.75	0.84	4.8	72.6
4	33.9	1.79	0.85	4.9	70.8
5	32.1	1.63	0.78	5.6	60.3
6	32.7	1.77	0.86	5.1	71.1

3.4. Chemical chractarization of raw and esterified upgraded bio-oils

In this study, the chemical composition of bio-oil from each experimental run was analyzed using Gas Chromatography-Mass Spectrometry (GC/MS). The compounds with the most prominent peak areas were selected, integrated, and quantitatively determined based on their area percentages.

 doi:10.20944/preprints202312.1065.v1

The analysis revealed that the chemical compositions of the esterified bio-oils produced in each experiment (Exp.1, Exp.2, Exp.3, Exp.4, Exp.5, and Exp.6) using the same experimental conditions were similar, though with differing peak intensities. Table 5 outlines the major compounds detected in the GC/MS analysis of both raw and esterified upgraded bio-oils employing five different catalysts and the AcB support, all processed at 300°C. The table distinctly demonstrates that all five bimetallic oxide catalysts, supported on activated rice straw biochar (CuO-Fe_3O_4/AcB) in Exp.2, Exp.3, Exp.4, Exp.5, and Exp.6, induced significant changes in the chemical composition of the esterified bio-oil compared to the raw bio-oil. Conversely, the chemical compounds found in the raw bio-oil were predominantly oxygenated compounds resulting from the thermal conversion of rice straw biomass to bio-oil. These identified chemical products closely resemble those reported in the literature concerning fast pyrolysis of raw bio-oil, such as acids, aldehydes, ketones, esters, furans, and phenols [51]. Notably, the primary chemical compounds identified in this upgrading experiment were esters appearing at specific retention times (2.71, 5.41, 8.86, 37.1, and 39.92) minutes, including ethyl acetate, ethyl propionate, ethyl butyrate, ethyl palmitate, and ethyl oleate, respectively (as detailed in Table 4) with Figure 6 confirming this in the chromatogram. Moreover, a substantial decrease in the levels of acid compounds at specific retention times (1.57, 2.68, 12.66, 36.61, and 39.48) was observed, corresponding to formic acid, acetic acid, 4-hydroxybutanoic acid, palmitic acid, and oleic acid, respectively The absence of esterified compounds in raw rice straw bio-oils and their presence in the upgraded products (Exp.2, Exp.3, Exp.4, Exp.5, and Exp.6) clearly indicates the occurrence of esterification reactions between the carboxylic acid groups and supercritical ethanol in the presence of acid catalyst or support. Additionally, in all upgrading experiments, formic acid and oleic acid were completely absent at specific retention times 1.57 and 39.48, respectively. Figure 7 validates this finding, showing the non-existence of esters in the raw rice straw bio-oil but their presence at varied concentrations in the experiments. It's significant to note that in Exp.4, Exp.5, and Exp.6 with a Cu: Fe ratio of 3:1, the ester yields were notably higher at 47.34%, 48.57%, and 46.57% respectively, in terms of chemical composition compared to the other experiments as presented in Tables 5. Conversely, phenolic compounds experienced a slight reduction in these three experiments compared to the rest. Exp.5 displayed the highest conversion of carboxylic acids into esters during the upgrading process, representing a substantial 90.4% conversion, leading to a reduced acidity in the esterified oil. This esterification also resulted in an increase in esters from 0.0% to 48.57%, along with a minor decrease in phenolic compound from 27.32% to 25.54% in comparison with the raw bio-oil, with selectivity towards ethyl acetate.

Therefore, Exp.5 serves as the optimal condition for effectively esterifying rice straw bio-oil in supercritical ethanol. These findings indicate that ester formation might be the primary cause reducing the bio-oil acidity, evident in both pH increase from 23.2% and TAN values decrease decreased by 28.1%. The reduction in oxygenated compounds, acid content, and increase in esters indicate the catalyst's excellent activity, consequently reducing viscosity and, thereby, the hydrophilicity of the final product [19]. In contrast to acids, esters display a greater promise in fuel composition, owing to their reduced corrosive impact on the engine surface. Ester formation is potentially a result of an esterification reaction between bio-oil acids and alcohol [52]. These changes not only boost stability but also improve the potential for blending hydrocarbons into the upgraded bio-oil. The enhanced levels of ethers and esters in the upgraded bio-oil strengthen it, attributed to a substantial drop in acids and aldehydes. Finally, the properties of the upgraded bio-oil experience a marked enhancement [53].

 doi:10.20944/preprints202312.1065.v1

Table 5. Compounds detected and identified by GC–MS of raw and esterified bio-oil.

RT (min)	Compound Name	(Area %)						
		Raw Bio-oil	EXP 1	EXP 2	EXP 3	EXP 4	EXP 5	EXP 6
	Acids							
1.57	Formic acid	2.14	0.00	0.00	0.00	0.00	0.00	0.00
2.68	Acetic acid	32.32	11.02	6.62	10.29	6.27	2.08	6.27
12.66	4-hydroxybutanoic acid	2.06	0.00	3.03	0.00	2.44	2.03	2.42
36.61	Palmitic acid	3.59	1.86	0.00	1.56	0.00	0.00	0.00
39.48	Oleic acid	2.57	0.00	0.00	0.00	0.00	0.00	0.00
	Total	42.68	12.88	9.65	11.85	8.71	4.11	8.69
	Ketones							
1.49	Acetone	0.00	1.90	0.00	1.87	1.98	4.12	2.01
3.87	1-hydroxypropan-2-one	11.65	0.00	0.00	0.00	0.00	0.00	0.00
7.50	1-hydroxy-2-butanone	1.82	0.00	0.00	0.00	0.00	0.00	0.00
9.93	Cyclopent-2-en-1-one	2.29	0.00	0.00	0.00	0.00	0.00	0.00
12.50	2-methylcyclopent-2-en-1-one	0.00	3.68	3.18	3.01	2.84	2.80	3.19
14.41	3-methylcyclopent-2-en-1-one	1.99	3.45	2.31	2.48	2.21	2.15	2.26
16.30	3-methylcyclopentane-1,2-dione	5.31	0.00	0.00	0.00	0.00	0.00	0.00
16.60	2,3-dimethylcyclopent-2-en-1-one	0.00	2.06	3.46	3.70	3.52	3.35	3.84
17.29	3,4,4-trimethylcyclopent-2-en-1-one	0.00	2.49	2.11	1.81	1.36	1.49	0.00
	Total	23.06	13.58	11.06	12.87	11.91	13.91	11.3
	Phenolics							
14.79	Phenol	3.30	5.97	4.19	4.52	4.64	4.73	4.54
17.03	*o*-cresol	2.76	3.52	2.71	2.79	2.90	2.48	5.57
17.63	*p*-Cresol	2.23	2.81	2.27	2.41	3.02	2.53	0.00
18.04	2-methoxyphenol	4.07	8.17	5.86	5.08	5.24	4.75	5.17
20.11	4-ethylphenol	2.49	5.43	4.27	3.89	4.49	3.84	4.04
20.82	3-ethoxyphenol	5.02	5.44	5.03	3.68	3.17	2.90	3.13
22.96	4-ethyl-2-methoxyphenol	2.50	4.48	3.52	2.62	2.99	2.13	2.68
24.64	2,6-dimethoxyphenol	2.70	0.00	2.04	0.00	0.00	0.00	0.00
25.32	4-Ethylcatechol	2.25	2.53	2.41	1.71	0.00	2.04	1.50
	Total	27.32	38.35	32.3	26.7	26.45	25.4	26.63
	Alcohols							
18.33	Cyclopropylmethanol	2.81	0.00	0.00	0.00	0.00	0.00	0.00
	Total	2.81	0.00	0.00	0.00	0.00	0.00	0.00
	Esters							
2.71	Ethyl acetate	0.00	16.67	24.83	27.69	33.89	36.55	32.55
5.41	Ethyl propionate	0.00	2.76	5.98	7.04	6.99	7.59	7.46
8.86	Ethyl butyrate	0.00	0.00	1.02	1.20	1.49	1.52	1.40
37.13	Ethyl palmitate	0.00	4.24	3.34	3.19	3.22	3.04	3.15
39.92	Ethyl oleate	0.00	2.48	1.62	1.82	1.75	1.39	2.01
	Total	0.00	26.15	36.79	40.94	47.34	48.57	46.57
	Ethers							
1.54	Ethoxyethane	2.22	1.77	2.10	3.25	1.67	3.91	2.09
	Total	2.22	1.77	2.10	3.25	1.67	3.91	2.09
	Others							
21.44	2,3-dihydrobenzofuran	1.91	2.19	0.00	0.00	0.00	0.00	0.00
17.76	Isobutyric anhydride	0.00	5.08	8.10	4.39	3.92	4.10	4.72
	Total	1.91	7.27	8.1	4.39	3.92	4.1	4.72

Preprints (www.preprints.org) | NOT PEER-REVIEWED | Posted: 14 December 2023 doi:10.20944/preprints202312.1065.v1

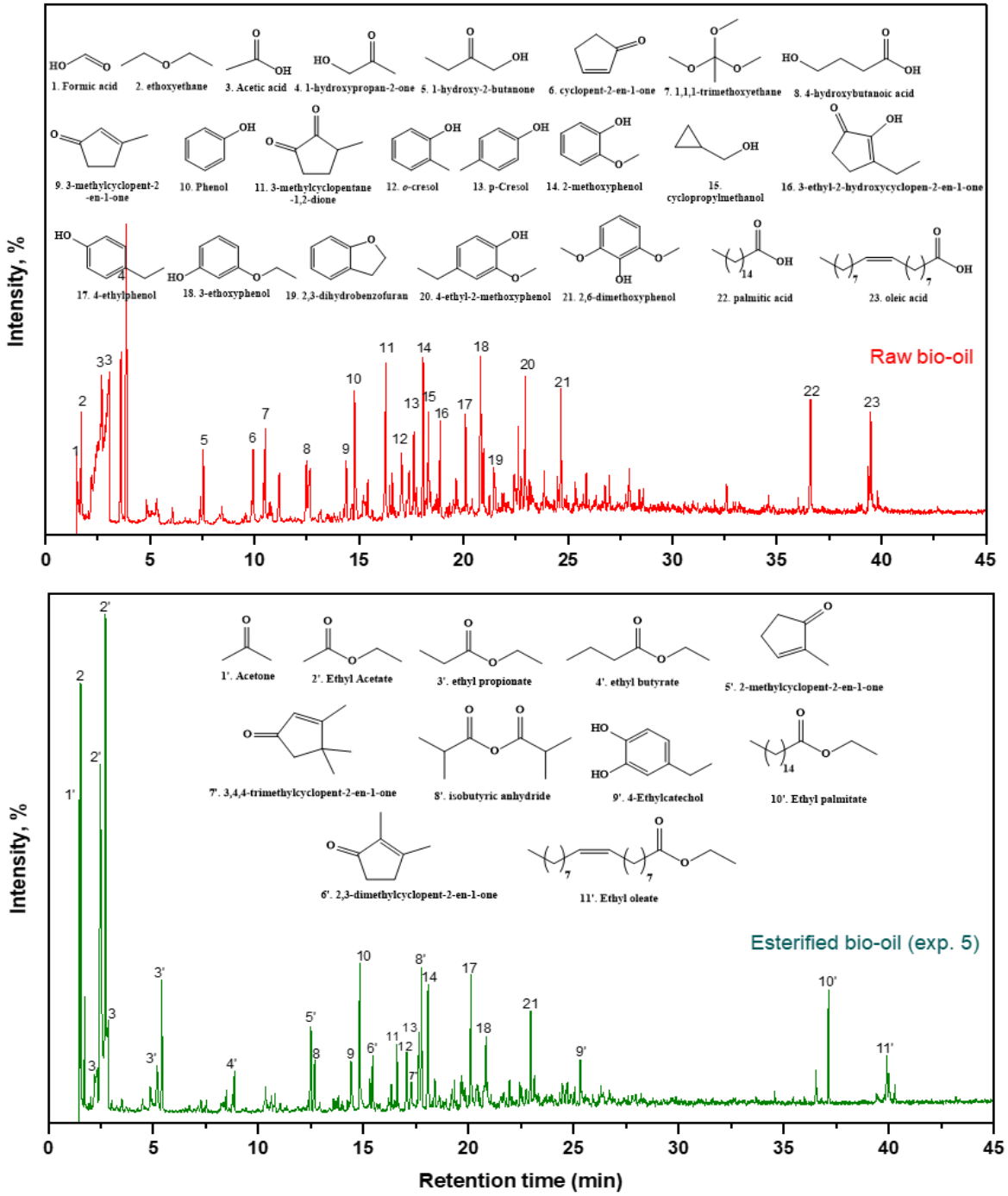

Figure 6. GC/MS chromatograms of raw and esterified bio-oils (Exp. 5).

Preprints (www.preprints.org) | NOT PEER-REVIEWED | Posted: 14 December 2023 doi:10.20944/preprints202312.1065.v1

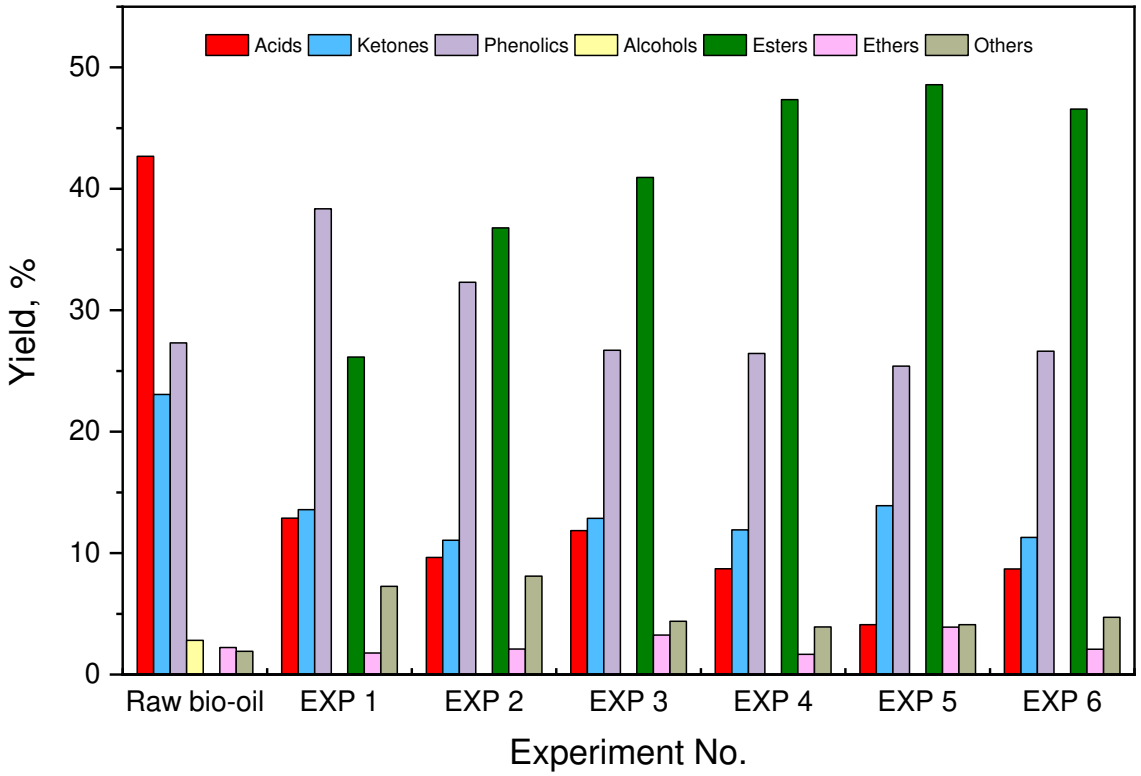

Figure 7. Yields of chemical compounds in raw and esterified bio-oils.

5. Conclusions

This study focused on enhancing bio-oil using upgrading methods involving supercritical ethanol. Bimetallic oxide catalysts supported on activated rice straw biochar (CuO-Fe_3O_4/AcB) were prepared with different Cu: Fe ratios. The application of these catalysts during supercritical ethanol-based upgrading resulted in significant enhancements in both physical and chemical properties of the bio-oil. Esterification, transesterification, and hydrogenation were identified as the key reactions contributing to this improvement. The elemental analysis results revealed an increase in carbon and hydrogen content due to the substantial hydrocarbon content in ethanol after blending, while the oxygen content in the bio-oil decreased. Analysis of the bio-oil's physical properties indicated the removal of acids during upgrading, leading to a pH increase because of the esterification capacity of supercritical ethanol, facilitated by the presence of newly formed esters. Also, all upgraded bio-oils experiment showed lower TAN values, viscosity, water content, and density compared to raw bio-oil. The higher heating value (HHV) of the bio-oil reached to 32.1 MJ/kg, approaching the value of conventional biodiesel fuel (36.4 MJ/kg). GC/MS chemical analysis showed that the bio-oil upgrading did not only improve bio-oil quality by decreasing oxygen-containing compounds and increasing calorific value, but also transformed the abundant carboxylic acids into esters, primarily ethyl acetate. The production of esters from the significant carboxylic acid reservoir addresses its corrosive nature and further enhances bio-oil's utility. Ethyl acetate, a prominent ester, offers several key advantages, including its favorable physicochemical properties, making it a valuable target for sustainable biofuel production. This research not only showcases innovative upgrading techniques, but also underscores their potential to revolutionize agricultural residue management, fostering cleaner energy production.

Author Contributions: Conceptualization, E. H., and I. E.; design and simulation, A. I., I. E., and E. H.; experiment and analysis, A. I., I. E., and E. H.; manuscript preparation, A. I., and E. H..; revision, E. H., and I. E.; supervision, E. H. All authors have read and agreed to the published version of the manuscript.

Funding: This paper is based on work supported by the U.S. - Egypt Science and Technology Joint Fund (The National Academy of Sciences (NAS) Award # SCON-10000558). This publication is also supported by the McIntire Stennis project under accession number 70011735.

Data Availability Statement: There are no data to provide.

Acknowledgments: This manuscript is publication #SB1120 of the Sustainable Bioproducts, Mississippi State University. This publication is also a contribution of the Forest and Wildlife Research Center, Mississippi State.

Conflicts of Interest: The authors declare no conflict of interest.

References

1. Jin, Y.; Hu, S.; Zhang, Z.; Zhu, B.; Bai, D. The path to carbon neutrality in China: A paradigm shift in fossil resource utilization. *Resources Chemicals and Materials* **2022**, *1*, 129-135, doi:10.1016/j.recm.2022.01.003.
2. Shamoon, A.; Haleem, A.; Bahl, S.; Javaid, M.; Bala Garg, S.; Chandmal Sharma, R.; Garg, J. Environmental impact of energy production and extraction of materials - a review. *Materials Today: Proceedings* **2022**, *57*, 936-941, doi:10.1016/j.matpr.2022.03.159.
3. Mohan, D.; Pittman, C.U.; Steele, P.H. Pyrolysis of wood /biomass for Bio-oil. *Progress in Energy and Combustion Science* **2017**, *62*, 848-889, doi:10.1021/ef0502397.
4. Shafie, S.M.; Masjuki, H.H.; Mahlia, T.M.I. Life cycle assessment of rice straw-based power generation in Malaysia. *Energy* **2014**, *70*, 401-410, doi:10.1016/j.energy.2014.04.014.
5. Sarangi, P.K.; Shadangi, K.P.; Srivastava, R.K. Chapter 5 - Agricultural waste to fuels and chemicals. **2023**, 87-98, doi:10.1016/B978-0-323-98363-1.00011-9.
6. Ahmad, R.; Hamidin, N. Bio-oil Product from Non-catalytic and Catalytic Pyrolysis of Rice Straw. *Australian Journal of Basic and Applied Sciences* **2013**, *7*, 61-65.
7. Oasmaa, A.; Lehto, J.; Solantausta, Y.; Kallio, S. Historical Review on VTT Fast Pyrolysis Bio-oil Production and Upgrading. *Energy and Fuels* **2021**, *35*, doi:10.1021/acs.energyfuels.1c00177.
8. Czernik, S.; Bridgwater, A.V. Overview of applications of biomass fast pyrolysis oil. *Energy and Fuels* **2004**, *18*, 590-598, doi:10.1021/ef034067u.
9. Patel, M.; Kumar, A. Production of renewable diesel through the hydroprocessing of lignocellulosic biomass-derived bio-oil: A review. *Renewable and Sustainable Energy Reviews* **2016**, *58*, 1293-1307, doi:10.1016/j.rser.2015.12.146.
10. Eschenbacher, A.; Fennell, P.; Jensen, A.D. A Review of Recent Research on Catalytic Biomass Pyrolysis and Low-Pressure Hydropyrolysis. *Energy and Fuels* **2021**, *35*, 18333-18369, doi:10.1021/acs.energyfuels.1c02793.
11. Kim, T.-S.; Kim, J.-Y.; Kim, K.-H.; Lee, S.; Choi, D.; Choi, I.-G.; Choi, J.W. The effect of storage duration on bio-oil properties. *Journal of Analytical and Applied Pyrolysis* **2012**, *95*, 118-125.
12. Maneechakr, P.; Karnjanakom, S. Improving the Bio-Oil Quality via Effective Pyrolysis/Deoxygenation of Palm Kernel Cake over a Metal (Cu, Ni, or Fe)-Doped Carbon Catalyst. *ACS Omega* **2021**, *6*, 20006-20014, doi:10.1021/acsomega.1c02999.
13. Hassan, E.B.M.; Steele, P.H.; Ingram, L. Characterization of fast pyrolysis bio-oils produced from pretreated pine wood. *Applied Biochemistry and Biotechnology* **2009**, *154*, 182-192, doi:10.1007/s12010-008-8445-3.
14. Kazmi, W.W.; Park, J.-Y.; Amini, G.; Lee, I.-G. Upgrading of esterified bio-oil from waste coffee grounds over MgNiMo/activated charcoal in supercritical ethanol. *Fuel Processing Technology* **2023**, *250*, 107915.
15. Kastner, J.R.; Miller, J.; Geller, D.P.; Locklin, J.; Keith, L.H.; Johnson, T. Catalytic esterification of fatty acids using solid acid catalysts generated from biochar and activated carbon. *Catalysis Today* **2012**, *190*, 122-132.
16. Monteiro, R.R.C.; dos Santos, I.A.; Arcanjo, M.R.A.; Cavalcante, C.L.; de Luna, F.M.T.; Fernandez-Lafuente, R.; Vieira, R.S. Production of Jet Biofuels by Catalytic Hydroprocessing of Esters and Fatty Acids: A Review. *Catalysts* **2022**, *12*, doi:10.3390/catal12020237.
17. Lee, J.-H.; Lee, I.-G.; Park, J.-Y.; Lee, K.-Y. Efficient upgrading of pyrolysis bio-oil over Ni-based catalysts in supercritical ethanol. *Fuel* **2019**, *241*, 207-217.
18. Shafaghat, H.; Kim, J.M.; Lee, I.-G.; Jae, J.; Jung, S.-C.; Park, Y.-K. Catalytic hydrodeoxygenation of crude bio-oil in supercritical methanol using supported nickel catalysts. *Renewable Energy* **2019**, *144*, 159-166.
19. Baloch, H.A.; Nizamuddin, S.; Siddiqui, M.T.H.; Riaz, S.; Konstas, K.; Mubarak, N.M.; Srinivasan, M.P.; Griffin, G.J. Catalytic upgradation of bio-oil over metal supported activated carbon catalysts in sub-supercritical ethanol. *Journal of Environmental Chemical Engineering* **2021**, *9*, doi:10.1016/j.jece.2021.105059.
20. Bagnato, G.; Sanna, A.; Paone, E.; Catizzone, E. Recent catalytic advances in hydrotreatment processes of pyrolysis bio-oil. *Catalysts* **2021**, *11*, 1-19, doi:10.3390/catal11020157.
21. Park, J.-Y.; Jeon, W.; Lee, J.-H.; Nam, B.; Lee, I.-G. Effects of supercritical fluids in catalytic upgrading of biomass pyrolysis oil. *Chemical Engineering Journal* **2019**, *377*, 120312.

22. Chen, W.; Luo, Z.; Yu, C.; Li, G.; Yang, Y.; Zhang, H. Upgrading of bio-oil in supercritical ethanol: Catalysts screening, solvent recovery and catalyst stability study. *Journal of Supercritical Fluids* **2014**, *95*, 387-393, doi:10.1016/j.supflu.2014.09.041.
23. Wen, D.; Jiang, H.; Zhang, K. Supercritical fluids technology for clean biofuel production. *Progress in Natural Science* **2009**, *19*, 273-284, doi:10.1016/j.pnsc.2008.09.001.
24. Wang, F.; Xu, J.; Jiang, J.; Liu, P.; Li, F.; Ye, J.; Zhou, M. Hydrotreatment of vegetable oil for green diesel over activated carbon supported molybdenum carbide catalyst. *Fuel* **2018**, *216*, 738-746, doi:10.1016/j.fuel.2017.12.059.
25. Wu, L.; Hu, X.; Wang, S.; Hasan, M.D.M.; Jiang, S.; Zhang, L.; Li, C.-Z. Reaction behaviour of light and heavy components of bio-oil in methanol and in water. *Fuel* **2018**, *232*, 645-652.
26. Hu, X.; Gunawan, R.; Mourant, D.; Hasan, M.D.M.; Wu, L.; Song, Y.; Lievens, C.; Li, C.-Z. Upgrading of bio-oil via acid-catalyzed reactions in alcohols—A mini review. *Fuel processing technology* **2017**, *155*, 2-19.
27. Ardiyanti, A.R.; Gutierrez, A.; Honkela, M.L.; Krause, A.O.I.; Heeres, H.J. Hydrotreatment of wood-based pyrolysis oil using zirconia-supported mono-and bimetallic (Pt, Pd, Rh) catalysts. *Applied Catalysis A: General* **2011**, *407*, 56-66.
28. Davidson, M.; Ji, Y.; Leong, G.J.; Kovach, N.C.; Trewyn, B.G.; Richards, R.M. Hybrid mesoporous silica/noble-metal nanoparticle materials—synthesis and catalytic applications. *ACS Applied Nano Materials* **2018**, *1*, 4386-4400.
29. Setiabudi, H.; Aziz, M.; Abdullah, S.; Teh, L.; Jusoh, R. Hydrogen production from catalytic steam reforming of biomass pyrolysis oil or bio-oil derivatives: A review. *International Journal of Hydrogen Energy* **2020**, *45*, 18376-18397.
30. Ren, X.-Y.; Cao, J.-P.; Zhao, X.-Y.; Yang, Z.; Liu, T.-L.; Fan, X.; Zhao, Y.-P.; Wei, X.-Y. Catalytic upgrading of pyrolysis vapors from lignite over mono/bimetal-loaded mesoporous HZSM-5. *Fuel* **2018**, *218*, 33-40.
31. Nava, R.; Pawelec, B.; Castaño, P.; Álvarez-Galván, M.C.; Loricera, C.V.; Fierro, J.L.G. Upgrading of bio-liquids on different mesoporous silica-supported CoMo catalysts. *Applied Catalysis B: Environmental* **2009**, *92*, 154-167.
32. Bu, Q.; Lei, H.; Zacher, A.H.; Wang, L.; Ren, S.; Liang, J.; Wei, Y.; Liu, Y.; Tang, J.; Zhang, Q.; et al. A review of catalytic hydrodeoxygenation of lignin-derived phenols from biomass pyrolysis. *Bioresource Technology* **2012**, *124*, 470-477, doi:10.1016/j.biortech.2012.08.089.
33. Kaewmeesri, R.; Nonkumwong, J.; Kiatkittipong, W.; Laosiripojana, N.; Faungnawakij, K. Deoxygenations of palm oil-derived methyl esters over mono- And bimetallic NiCo catalysts. *Journal of Environmental Chemical Engineering* **2021**, *9*, doi:10.1016/j.jece.2021.105128.
34. Liu, R.; Rahman, M.M.; Sarker, M.; Chai, M.; Li, C.; Cai, J. A review on the catalytic pyrolysis of biomass for the bio-oil production with ZSM-5: Focus on structure. *Fuel processing technology* **2020**, *199*, 106301.
35. Sihombing, J.L.; Herlinawati, H.; Pulungan, A.N.; Simatupang, L.; Rahayu, R.; Wibowo, A.A. Effective hydrodeoxygenation bio-oil via natural zeolite supported transition metal oxide catalyst. *Arabian Journal of Chemistry* **2023**, *16*, 104707.
36. Ruan, C.; Akutsu, R.; Yang, K.; Zayan, N.M.; Dou, J.; Liu, J.; Bose, A.; Brody, L.; Lamb, H.H.; Li, F. Hydrogenation of bio-oil-derived oxygenates at ambient conditions via a two-step redox cycle. *Cell Reports Physical Science* **2023**, *4*.
37. Chen, C.; Ling, H.; Wei, D.; Wei, Y.; Fan, D.; Zhao, J. Microwave catalytic co-pyrolysis of chlorella vulgaris and oily sludge by nickel-X (X= Cu, Fe) supported on activated carbon: Characteristic and bio-oil analysis. *Journal of the Energy Institute* **2023**, 101401.
38. Zhang, J.; Chen, B.; Ge, Y.; Li, Z. Efficient depolymerization of alkali lignin to monophenols using one-step synthesized Cu–Ni bimetallic catalysts inlaid in homologous biochar. *Biomass and Bioenergy* **2023**, *175*, 106873.
39. Zhang, M.; Han, X.; Wang, H.; Zeng, Y.; Xu, C.C. Hydrodeoxygenation of Pyrolysis Oil in Supercritical Ethanol with Formic Acid as an In Situ Hydrogen Source over NiMoW Catalysts Supported on Different Materials. *Sustainability (Switzerland)* **2023**, *15*, doi:10.3390/su15107768.
40. Cai, T.; Liu, X.; Zhang, J.; Tie, B.; Lei, M.; Wei, X.; Peng, O.; Du, H. Silicate-modified oiltea camellia shell-derived biochar: A novel and cost-effective sorbent for cadmium removal. *Journal of Cleaner Production* **2021**, *281*, doi:10.1016/j.jclepro.2020.125390.
41. Lee, J.; Kim, K.-H.; Kwon, E.E. Biochar as a Catalyst. *Renewable and Sustainable Energy Reviews* **2017**, *77*, 70-79, doi:10.1016/j.rser.2017.04.002.
42. Ma, J.F.; Tamai, K.; Ichii, M.; Wu, G.F. A rice mutant defective in Si uptake. *Plant Physiology* **2002**, *130*, 2111-2117, doi:10.1104/pp.010348.
43. Nejati, B.; Adami, P.; Bozorg, A.; Tavasoli, A.; Mirzahosseini, A.H. Catalytic pyrolysis and bio-products upgrading derived from Chlorella vulgaris over its biochar and activated biochar-supported Fe catalysts. *Journal of Analytical and Applied Pyrolysis* **2020**, *152*, doi:10.1016/j.jaap.2020.104799.

44. Luo, Y.; Hassan, E.B.; Miao, P.; Xu, Q.; Steele, P.H. Effects of single-stage syngas hydrotreating on the physical and chemical properties of oxidized fractionated bio-oil. *Fuel* **2017**, *209*, 634-642, doi:10.1016/j.fuel.2017.07.114.
45. Zhu, L.; Zhao, N.; Tong, L.; Lv, Y. Structural and adsorption characteristics of potassium carbonate activated biochar. *RSC Advances* **2018**, *8*, 21012-21019, doi:10.1039/c8ra03335h.
46. Liu, Y.; Li, Z.; Leahy, J.J.; Kwapinski, W. Catalytically upgrading bio-oil via esterification. *Energy and Fuels* **2015**, *29*, 3691-3698, doi:10.1021/acs.energyfuels.5b00163.
47. Yuan, G.Q.; Jiang, H.F.; Lin, C.; Liao, S.J. Shape- and size-controlled electrochemical synthesis of cupric oxide nanocrystals. *Journal of Crystal Growth* **2007**, *303*, 400-406, doi:10.1016/j.jcrysgro.2006.12.047.
48. Chandrappa, K.G.; Venkatesha, T.V. Generation of nanostructured CuO by electrochemical method and its Zn–Ni–CuO composite thin films for corrosion protection. *Materials and corrosion* **2013**, *64*, 831-839.
49. Elsayed, I.; Jackson, M.A.; Hassan, E.B. Hydrogen-Free Catalytic Reduction of Biomass-Derived 5-Hydroxymethylfurfural into 2,5-Bis(hydroxymethyl)furan Using Copper–Iron Oxides Bimetallic Nanocatalyst. *ACS Sustainable Chemistry & Engineering* **2020**, *8*, 1774-1785, doi:10.1021/acssuschemeng.9b05575.
50. Lachos-Perez, D.; Martins-Vieira, J.C.; Missau, J.; Anshu, K.; Siakpebru, O.K.; Thengane, S.K.; Morais, A.R.C.; Tanabe, E.H.; Bertuol, D.A. Review on Biomass Pyrolysis with a Focus on Bio-Oil Upgrading Techniques. *Analytica* **2023**, *4*, 182-205.
51. Li, H.; Xia, S.; Li, Y.; Ma, P.; Zhao, C. Stability evaluation of fast pyrolysis oil from rice straw. *Chemical Engineering Science* **2015**, *135*, 258-265, doi:10.1016/j.ces.2015.03.065.
52. Omar, S.; Alsamaq, S.; Yang, Y.; Wang, J. Production of renewable fuels by blending bio-oil with alcohols and upgrading under supercritical conditions. *Frontiers of Chemical Science and Engineering* **2019**, *13*, 702-717, doi:10.1007/s11705-019-1861-9.
53. Baloch, H.A.; Nizamuddin, S.; Siddiqui, M.T.H.; Riaz, S.; Konstas, K.; Mubarak, N.; Srinivasan, M.; Griffin, G. Catalytic upgradation of bio-oil over metal supported activated carbon catalysts in sub-supercritical ethanol. *Journal of Environmental Chemical Engineering* **2021**, *9*, 105059.